PHYSICAL REVIEW B **93**, 035308 (2016)

Poisson Green's function method for increased computational efficiency in numerical calculations of Coulomb coupling elements

Anke Zimmermann, Sandra Kuhn, and Marten Richter
Institut für Theoretische Physik, Nichtlineare Optik und Quantenelektronik, Technische Universität Berlin,
Hardenbergstrasse 36, EW 7-1, 10623 Berlin, Germany

(Received 30 July 2015; revised manuscript received 13 November 2015; published 19 January 2016)

Often, the calculation of Coulomb coupling elements for quantum dynamical treatments, e.g., in cluster or correlation expansion schemes, requires the evaluation of a six dimensional spatial integral. Therefore, it represents a significant limiting factor in quantum mechanical calculations. If the size or the complexity of the investigated system increases, many coupling elements need to be determined. The resulting computational constraints require an efficient method for a fast numerical calculation of the Coulomb coupling. We present a computational method to reduce the numerical complexity by decreasing the number of spatial integrals for arbitrary geometries. We use a Green's function formulation of the Coulomb coupling and introduce a generalized scalar potential as solution of a generalized Poisson equation with a generalized charge density as the inhomogeneity. That enables a fast calculation of Coulomb coupling elements and, additionally, a straightforward inclusion of boundary conditions and arbitrarily spatially dependent dielectrics through the Coulomb Green's function. Particularly, if many coupling elements are included, the presented method, which is not restricted to specific symmetries of the model, presents a promising approach for increasing the efficiency of numerical calculations of the Coulomb interaction. To demonstrate the wide range of applications, we calculate internanostructure couplings, such as the Förster coupling, and illustrate the inclusion of symmetry considerations in the method for the Coulomb coupling between bound quantum dot states and unbound continuum states.

DOI: 10.1103/PhysRevB.93.035308

I. INTRODUCTION

A microscopic analysis of the Coulomb coupling is essential for the understanding of several physical processes in condensed matter such as the scattering of charge carriers [1,2] or the formation of collective states like excitons and biexcitons [3,4]. Therefore, the Coulomb coupling is an important many particle interaction in a variety of systems such as nanostructures like quantum dots (QDs) or wells [1], coupled nanotubes [5,6], bulk semiconductors [2,7], and graphene [8,9], as well as atomic structures and molecular systems [10,11].

Typically, for the calculation of the Coulomb coupling in a spatially homogeneous system, the free space Coulomb potential $G(\boldsymbol{r},\boldsymbol{r}')_{\text{free}} = 1/(4\pi\varepsilon_0\varepsilon_r|\boldsymbol{r}-\boldsymbol{r}'|)$ is used [12,13]. Therefore, a six dimensional spatial integral is evaluated for the matrix elements of the two-particle interaction [14,15] including electron wave functions. The fast computation of Coulomb coupling elements is an important factor in electronic structure calculations [11,16] as well as for quantum dynamics [17,18] and efficient density matrix calculations using many-body correlation expansions [19,20].

Systems involving only a few electronic levels have been investigated in detail in quantum dynamical calculations, this includes, e.g., QD interband transitions [5] and their modifications due to a dielectric medium [21]. For larger or asymmetric complex systems, the numerical computation of the Coulomb coupling constitutes a significant limiting factor and, therefore, approaches to efficiently calculate the Coulomb interaction are needed. Often, a radial symmetry is exploited and spherical coordinates are used to simplify the spatial integrals. Thus the Coulomb potential can be expressed by Legendre polynomials [13,22]. In Ref. [23], spherical coordinates were used to calculate the Coulomb interaction of a molecular complex, which is influenced by the presence of an adjunct metal nanoparticle. Typically, in quantum dynamical calculations of QD systems, several analytic approaches for evaluating the Coulomb interaction are based on the symmetries of the QD confinement [4,5,24] and the shape of the electron wave functions [2].

If the system includes the calculation of a high number of coupling elements, the resulting computational constraints [11,13] require an efficient model to calculate the Coulomb coupling elements numerically. In Ref. [11], a generalization of a multipole expansion [25] was presented for electronic structure calculations (e.g., for large molecules) to reduce the numerical effort for an increasing system size. For the Coulomb coupling involving continuum states, which influence dephasing [26] and scattering processes [27,28] as well as the formation of excitons between carriers of the QD and the continuum [29], a high number of coupling elements occurs. In addition, many Coulomb elements need to be calculated for varying distances between the nanostructures, since the Coulomb coupling between carriers of spatially separated systems (e.g., coupled QDs [30]) depends on the distance.

A method for an efficient numerical calculation of Coulomb coupling elements is given by a transformation of the electron wave functions into the Fourier space. The Fourier transformation can be used to separate the integrals of the two-particle Coulomb interaction, if the Coulomb potential for a homogenous medium in free space is considered [6,13,31]. In real space, the connection of the electron wave functions with the Coulomb potential results in a six dimensional integral. In contrast, in Fourier domain, the Coulomb coupling for a spatially homogenous medium is simply given as product of the electron wave functions and the Coulomb potential. That requires the calculation of a threefold integral and additionally, three dimensional Fourier transformations, respectively. Compared to a six dimensional integral in real space, the numerical complexity is reduced in the Fourier domain. However, a singularity of the Coulomb potential is also present in Fourier space and the Fourier transformation cannot be applied with the same numerical reduction for spatially inhomogeneous dielectrics.

For nanostructures such as QDs, a calculation of the Coulomb coupling in Fourier domain often includes form factors, which are defined by a Fourier transformation of the product of two electron wave functions. For example, in Ref. [13], form factors were introduced to calculate the Coulomb matrix elements between exciton and biexciton states for the impact ionization in semiconductor nanocrystals with surface polarization. In Ref. [2], form factors of an in-plane Fourier transformation and the construction of orthogonal plane waves [14] were used to simplify the calculation of the Coulomb coupling between a QD and a wetting layer. In the spherical symmetric case, the form factors can be formulated using spherical coordinates in the Fourier domain [5] to further reduce the computational costs.

In contrast, this paper presents a numerical method for an efficient calculation of Coulomb coupling elements in real space, which is not restricted to specific symmetry properties of the permittivity or the whole system. The method naturally includes the screening introduced through a spatially dependent permittivity. We reduce the computational complexity by decreasing the dimension of the spatial integrals, required for the calculation of Coulomb coupling elements. This is achieved by using a Green's function formulation of the Coulomb potential [32,33]. We identify a generalized scalar potential as a solution of the generalized Poisson equation with a generalized charge density as the inhomogeneity, determined by the complex electron wave functions.

Since solvers and libraries such as PETSc [34] for an efficient numerical computation of partial differential equations [35,36] are available, a calculation of the Coulomb potential based on the solution of a differential equation is feasible with a straightforward implementation. Furthermore, solving a modified Poisson equation offers the possibility of including screening effects as well as the influence of a spatially dependent dielectric function $\varepsilon(\boldsymbol{r})$ [15]. In this way, induced surface charge effects, which can result in energetic shifts [32] (e.g., for the band gap and exciton resonances), can be included by solving the Poisson differential equation with appropriate boundary conditions [15].

The Poisson Green's function (PGF) method, presented in this paper, is very general and allows an efficient calculation of Coulomb coupling elements without being restricted to a specific analytic expression of the Green's function or to particular system symmetries. We achieve a similar reduction in the numerical complexity as in a calculation of the Coulomb potential in Fourier domain using form factors, but without the restriction to the Coulomb potential in free space with a spatially homogenous dielectric constant ε_r.

Similar methods are already known and used by different authors in other contexts such as *ab initio* treatments and electronic structure calculations. In Ref. [33], a Green's function representation of the solution of a Poisson equation was introduced to calculate the screening of the classical interaction of electrons of a quantum dot with gate electrodes. Therefore, the Green's function is explicitly determined and the screened electrostatic energy in a dielectric material is calculated. In Refs. [12,37,38], the Coulomb potential is obtained from solving a Poisson equation to calculate the Coulomb energy in the context of electronic structure calculations. Especially for including the influence of a spatially inhomogeneous medium, a generalized Poisson equation can be introduced, as is done in Refs. [32,39]. Additionally, a Poisson equation can be used to reach a linear scaling of the Coulomb problem with the system size [40]. Furthermore, other methods exist, which include a Poisson equation to calculate many Coulomb coupling elements. For example, in Ref. [41], a method was introduced, based on the expansion of the charge density in a specific set of functions, to reduce the number of integrals required for the calculation of Coulomb interactions in the context of a density functional theory. Nevertheless, as far as we are aware, the method based on the Green's function formulation of a solution of a Poisson equation without the restriction to certain symmetries or an explicit Green's function and the wide range of applications is not yet discussed in the literature devoted to the quantum dot community. Therefore, in this paper, we present the PGF method for increasing the numerical efficiency in real space without being restricted to specific symmetries, e.g., of the quantum dot confinement potential or the electron wave functions, and without determining an explicit analytic Green's function.

To demonstrate the wide range of applications of the Poisson Green's function method, we present results of the Coulomb coupling for two QD systems (cf. Fig. 1), including the formation of excitonic states [22,42,43]. The first example model consists of two Coulomb coupled colloidal QDs and includes the monopole-monopole interaction as well as the Förster induced dipole-dipole coupling [22] [cf. Fig. 1(i)]. For demonstrating the feasibility of the approach, we calculate the Coulomb contributions connected to the monopole-monopole and dipole-dipole coupling without explicitly specifying the Green's function of the problem. Additionally, for self-organized QDs embedded in a host material, we calculate the Coulomb coupling for bound electron and hole QD states

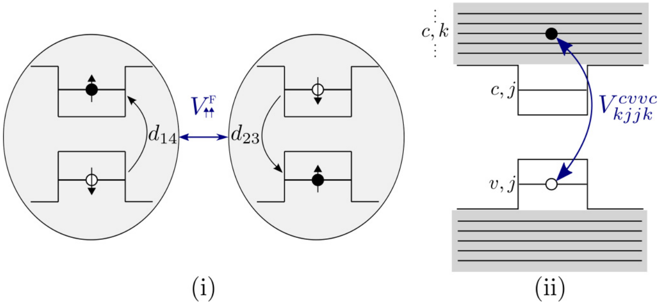

FIG. 1. Model schemes: (i) the Förster induced dipole-dipole Coulomb coupling between two QDs and (ii) the monopolelike coupling between a QD and many continuum states of the surrounding material.

coupled to many continuum states [29] [cf. Fig. 1(ii)]. Here we show that a drastic reduction of computational costs is also possible with the presented method, if typical symmetries, such as radial symmetry of the QD confinement potential, are included.

The paper is organized as follows. First, in Sec. II, the Coulomb Hamiltonian is derived using the Coulomb gauge representation of the scalar potential to understand the origin of Coulomb coupling. In Sec. III, the PGF method based on the solution of a generalized Poisson equation is presented for fast numerical calculations of the Coulomb coupling. To demonstrate the strength of the formalism for calculating many coupling elements, we present as example two applications of the method in real space: the position dependent inter-QD coupling between two QDs in Sec. IV and the coupling of a bound QD state to many continuum states in Sec. V.

II. COULOMB HAMILTONIAN

In this section, the Hamiltonian of the Coulomb interaction is derived for a spatially inhomogeneous medium [44]. Therefore, the Coulomb coupling elements are formulated using a Green's function representation of a Poisson equation as usual. The PGF method, presented in Sec. III, will include a Green's function formulation in an analogous way.

The inhomogeneous Maxwell equations describe electromagnetic fields, including free charges ρ and currents $\boldsymbol{j}$ as source terms [45]. To solve the Maxwell equations in material, we use the vector potential $\boldsymbol{A}$ in a generalized Coulomb gauge [45,46]: $\nabla_{\boldsymbol{r}} \cdot (\varepsilon(\boldsymbol{r})\boldsymbol{A}(\boldsymbol{r})) = 0$.

Following the approach of Ref. [32], in semiclassical description, the longitudinal part of the dielectric displacement is defined as $\boldsymbol{D}_L(\boldsymbol{r}) = -\varepsilon_0\varepsilon(\boldsymbol{r})\nabla_{\boldsymbol{r}}\Phi(\boldsymbol{r})$ with the scalar potential Φ. Therefore, the Coulomb field energy is given by

$$H_C = \frac{1}{2}\int d^3r \frac{\boldsymbol{D}_L(\boldsymbol{r}) \cdot \boldsymbol{D}_L(\boldsymbol{r})}{\varepsilon_0\varepsilon(\boldsymbol{r})}. \tag{1}$$

Inserting the definition of the longitudinal dielectric displacement $\boldsymbol{D}_L$ in Eq. (1), the scalar potential Φ appears:

$$H_C = -\frac{1}{2}\int d^3r\, \nabla_{\boldsymbol{r}}\Phi(\boldsymbol{r}) \cdot \boldsymbol{D}_L(\boldsymbol{r}). \tag{2}$$

After an integration by parts, the Maxwell equation $\nabla_{\boldsymbol{r}} \cdot \boldsymbol{D}_L(\boldsymbol{r}) = \rho(\boldsymbol{r})$ is used to include the free charge density ρ:

$$H_C = \frac{1}{2}\int d^3r\, \Phi(\boldsymbol{r})\rho(\boldsymbol{r}). \tag{3}$$

In the Coulomb gauge, the scalar potential Φ satisfies the Poisson equation and the influence of a spatially inhomogeneous medium is represented by a dielectric function $\varepsilon(\boldsymbol{r})$ [32,47]:

$$\nabla_{\boldsymbol{r}} \cdot (\varepsilon(\boldsymbol{r})\nabla_{\boldsymbol{r}}\Phi(\boldsymbol{r})) = -\frac{\rho(\boldsymbol{r})}{\varepsilon_0}. \tag{4}$$

To express the solution of Eq. (4) for a spatially inhomogeneous medium, as is done in Ref. [32], a generalized Coulomb Green's function $G(\boldsymbol{r},\boldsymbol{r}')$ is defined through

$$\nabla_{\boldsymbol{r}} \cdot (\varepsilon(\boldsymbol{r})\nabla_{\boldsymbol{r}}G(\boldsymbol{r},\boldsymbol{r}')) = -\frac{1}{\varepsilon_0}\delta(\boldsymbol{r}-\boldsymbol{r}'). \tag{5}$$

Using the definition of the Green's function in Eq. (5), the scalar potential Φ as solution of the Poisson Eq. (4) is

$$\Phi(\boldsymbol{r}) = \int d^3r' G(\boldsymbol{r},\boldsymbol{r}')\rho(\boldsymbol{r}'). \tag{6}$$

The scalar potential in the Hamiltonian in Eq. (3) is replaced using Eq. (6) and the two-particle Coulomb Hamiltonian is obtained:

$$H_C = \frac{1}{2}\int d^3r \int d^3r' \rho(\boldsymbol{r})G(\boldsymbol{r},\boldsymbol{r}')\rho(\boldsymbol{r}'). \tag{7}$$

In second quantization, the charge density is given by the electron field operators expanded into electronic eigenstates. Thus the Coulomb Hamiltonian is

$$H_{\mathrm{C}} = \frac{1}{2}\sum_{1234} V_{1234}a_1^\dagger a_2^\dagger a_3 a_4, \tag{8}$$

with 1, 2, 3, and 4 as multi-indices representing all quantum numbers states (e.g., band index, QD number, spin configuration) and $a_i^\dagger$ (a_i) denoting the creation (annihilation) operators for electrons of the state i. The Coulomb coupling elements V_{1234} of a generalized Coulomb interaction potential $G(\boldsymbol{r},\boldsymbol{r}')$ read [16,48]

$$V_{1234} = e^2\int d^3r \int d^3r' \phi_1^*(\boldsymbol{r})\phi_2^*(\boldsymbol{r}')G(\boldsymbol{r},\boldsymbol{r}')\phi_3(\boldsymbol{r}')\phi_4(\boldsymbol{r}), \tag{9}$$

where $\phi_i(\boldsymbol{r})$ is the electron wave function of the state i. In general, Eq. (9) requires a numerical solution. The six dimensional space integral needs to be evaluated for calculating the two-particle Coulomb interaction. Accordingly, the calculation of the Coulomb coupling elements is numerically demanding, compared to three dimensional integrals, and constitutes a significant limitation factor in the solution of complex problems.

Particularly, with regard to the computation of many Coulomb coupling elements, a method for fast numerical calculations is necessary. This paper gives a general numerical procedure to reduce the computational cost of the calculation of the related coupling elements in Eq. (9).

III. METHOD

Similar to the derivation of the Hamiltonian in Sec. II, the numerical efficient PGF method for a fast calculation of Coulomb coupling elements, presented in this section, is based on a Green's function representation of the solution of a generalized Poisson equation [33] [analogous to Eq. (4)]. The method, schematically illustrated in Fig. 2, reduces the high computational complexity of Eq. (9) by introducing a generalized scalar potential $\Phi_{23}(\boldsymbol{r})$, which includes the Green's function. This approach separates the number of integrals from a six dimensional integral in Eq. (9) to two separate three dimensional integrals:

$$V_{1234} = e\int d^3r\, \phi_1^*(\boldsymbol{r})\Phi_{23}(\boldsymbol{r})\phi_4(\boldsymbol{r}). \tag{10}$$

Thus, to reproduce the Coulomb coupling element formula of Eq. (9), the scalar potential $\Phi_{23}(\boldsymbol{r})$ is given by

$$\Phi_{23}(\boldsymbol{r}) = e\int d^3r' \phi_2^*(\boldsymbol{r}')G(\boldsymbol{r},\boldsymbol{r}')\phi_3(\boldsymbol{r}'). \tag{11}$$

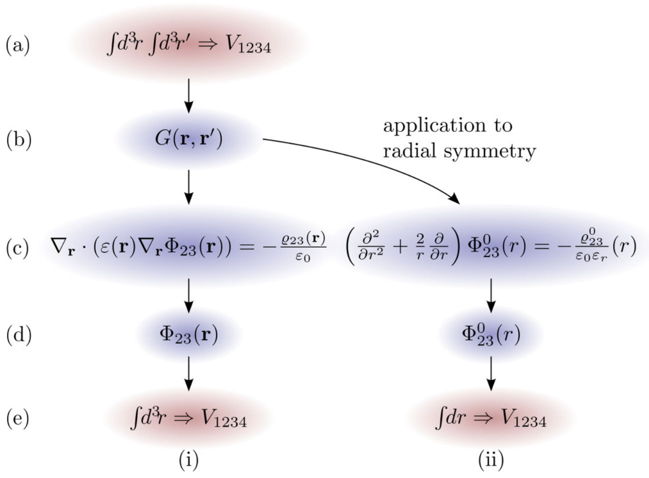

FIG. 2. PGF method for increasing the efficiency in numerical calculations of Coulomb coupling elements. (i) Typically, the calculation of (a) the Coulomb interaction includes a six dimensional integral. Using (b) the Green's function formalism, (c) a generalized Poisson equation is formulated to calculate (d) the scalar potential. Therefore, (e) the number of integrals is reduced. (ii) In the case of radial symmetry, (c) the radial part of the Laplace operator in spherical coordinates is used to calculate (d) the radial scalar potential and (e) a one dimensional integral is evaluated for calculating Coulomb elements.

The Green's function in Eq. (11) [Fig. 2(b)], which includes properties of the geometry [33], is determined by Eq. (5) in a dielectric medium with a spatially dependent dielectric function $\varepsilon(\boldsymbol{r})$ [15]. Following the derivation of the Hamiltonian in Sec. II, the generalized scalar potential, given by Eq. (11), can be identified as a Green's function representation of the solution of a generalized Poisson equation [33], analogous to Eq. (6):

$$\Phi_{23}(\boldsymbol{r}) = \int d^3r' G(\boldsymbol{r},\boldsymbol{r}')\varrho_{23}(\boldsymbol{r}'). \tag{12}$$

Therefore, the generalized charge density $\varrho_{23}(\boldsymbol{r})$, described by the corresponding electron wave functions [12], is introduced as $\varrho_{23}(\boldsymbol{r}) = e\phi_2^*(\boldsymbol{r})\phi_3(\boldsymbol{r})$. Note that the electron wave functions may be complex. Thus the charge density $\varrho_{23}(\boldsymbol{r})$ and the scalar potential $\Phi_{23}(\boldsymbol{r})$ may be complex as well and, therefore, they are not directly measurable but mathematical quantities, solely intended for the calculation of Coulomb coupling elements.

Accordingly, for applications in materials with spatially varying permittivities, a generalized Poisson equation determines the generalized scalar potential $\Phi_{23}(\boldsymbol{r})$ of the Coulomb interaction [4,39], analogous to Eq. (4), with a potentially complex charge density as the inhomogeneity; cf. Fig. 2(c)(i):

$$\nabla_{\boldsymbol{r}} \cdot (\varepsilon(\boldsymbol{r})\nabla_{\boldsymbol{r}}\Phi_{23}(\boldsymbol{r})) = -\frac{\varrho_{23}(\boldsymbol{r})}{\varepsilon_0}. \tag{13}$$

For example, if the dielectric constant of the system differs from that of the surrounding medium (e.g., a QD in a solvent), surface charge effects may be considered [21,43]. The PGF method offers the possibility of including such effects as appropriate geometries in $\varepsilon(\boldsymbol{r})$ or as boundary conditions for $\Phi_{23}(\boldsymbol{r})$ [49] by solving the generalized Poisson Eq. (13). To solve such a differential equation, e.g., finite-difference methods [39] or finite elements methods [50,51] can be used. Nowadays, solvers are very fast and highly optimized [35,36], so that together with an integration of Eq. (10) a fast calculation and implementation of the Coulomb coupling is accomplished.

In Refs. [32,33], the Green's function representation of a generalized Poisson equation is used to calculate the Coulomb interaction for applications in material by determining the Green's function explicitly. The numerical calculation of $\Phi_{23}(\boldsymbol{r})$ is applicable to a larger variety of systems than the derivation of a specialized analytic expressions. Therefore, we propose to solve the Poisson equation directly, without specifying the Green's function explicitly. Nevertheless, this reduces the numerical complexity of the six dimensional integral in Eq. (9) [cf. Fig. 2(i)].

The numerical effort for evaluating the integrals of the two-particle Coulomb interaction in Eq. (9) scales as $\mathcal{O}(N^6)$, where N is the number of grid points in one dimension assuming a cubic grid used to discretize the problem. In the PGF method, the three dimensional integral in Eq. (10), which scales with the system size $\mathcal{O}(N^3)$, needs to be evaluated during the calculation of Coulomb coupling elements. Additionally, the generalized scalar potential $\Phi_{23}(\boldsymbol{r})$, used to separate the integral expression in Eq. (9), is determined by the numerical solution of the Poisson Eq. (13). Due to the development of efficient solvers for differential equations, a linear scaling with the system size in three dimensions $\mathcal{O}(N^3)$ can be obtained [36,40,52], e.g., by using multigrid methods [53], which are also included in libraries such as PETSc [34].

A transformation into the Fourier space can be used to efficiently calculate the Coulomb coupling by separating the integrals of the two-particle Coulomb interaction in Fourier domain. For a spatially homogenous medium, the Coulomb coupling elements in Fourier domain are given as product of electron wave functions and the Coulomb potential. Therefore, the formalism of the Fourier transformation includes the evaluation of a three dimensional integral in Fourier space scaling as $\mathcal{O}(N^3)$ for the reciprocal grid. In addition, three dimensional Fourier transformations of the electron wave functions are needed to determine form factors [5,6]. Therefore, a fast Fourier transform [54] is used, which scales as $\mathcal{O}(N^3 \log N)$ [36,53,55]. In contrast to the transformation into the Fourier space, the presented PGF method is not restricted to the case of a homogeneous dielectric medium ε_r in free space [44] and, therefore, effects caused by a spatially dependent dielectric medium can be included. Furthermore, using the PGF method, singularities in the Green's function are avoided, which often increase the numerical costs.

If certain symmetries are available, e.g., for spherical symmetric systems [12,13], the scalar potential $\Phi_{23}(\boldsymbol{r})$ is calculated using Eq. (13) adapted to the symmetry, as illustrated in Fig. 2(ii) for the application of radial symmetry. This allows the symmetries, for example of radially symmetric systems, to be exploited with the presented PGF method.

Often, modifications of the Coulomb potential due to screening are necessary [31,56,57]. In the case of a homogeneous medium, the dielectric function ε_r is constant and, therefore, the left hand side of the Poisson Eq. (13) is given by the Laplace operator $\Delta_{\boldsymbol{r}}$ operating on the scalar potential $\Phi_{23}(\boldsymbol{r})$. Screening in the Yukawa form for homogeneous media may be included into the formula of the PGF method by introducing a constant screening factor α in the Poisson Eq. (13) with a constant dielectric function ε_r:

$$(\Delta_{\boldsymbol{r}} - \alpha^2)\Phi_{23}(\boldsymbol{r}) = -\frac{\varrho_{23}(\boldsymbol{r})}{\varepsilon_r\varepsilon_0}. \tag{14}$$

Therefore, the definition of the Green's function in Eq. (5) for an isotropic medium is adapted for screening by including the screening constant α:

$$(\Delta_{\boldsymbol{r}} - \alpha^2)G_\alpha(\boldsymbol{r},\boldsymbol{r}') = -\frac{1}{\varepsilon_r\varepsilon_0}\delta(\boldsymbol{r} - \boldsymbol{r}'). \tag{15}$$

Then, the PGF method can be applied straightforwardly using Eq. (10) and Eq. (12) to calculate screened Coulomb coupling elements in real space. The Yukawa potential $G_\alpha(\boldsymbol{r},\boldsymbol{r}') = e^{-\alpha|\boldsymbol{r}-\boldsymbol{r}'|}/(4\pi\varepsilon_0\varepsilon_r|\boldsymbol{r} - \boldsymbol{r}'|)$ with its Fourier transform $G_\alpha(\boldsymbol{q}) = 1/(\varepsilon_0\varepsilon_r(q^2 + \alpha^2))$, which is typically used to account for screening in semiconductors with a homogeneous medium [58] [cf. Eq. (15)], represents the Green's function.

In the following, we present a general approach for intersystem couplings in Sec. IV and an application for the radially symmetric case in Sec. V to demonstrate different applications of the presented PGF method in real space.

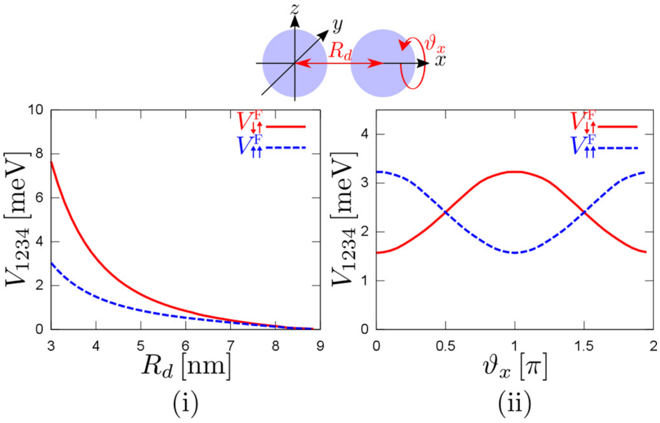

(i) (ii)

FIG. 3. Förster dipole-dipole coupling between two QDs as function of (i) the distance between the QDs and (ii) their orientation to each other. The interdot Coulomb coupling elements decay with increasing distance. The spin selective Förster coupling elements depend on the relative orientation of the QDs to each other. Therefore, many Coulomb coupling elements need to be calculated, if the spatial arrangement of the QDs is varying.

IV. INTER-QD COULOMB COUPLING

The PGF method for an efficient numerical calculation of Coulomb coupling elements [cf. Fig. 2(i)] does not rely on specific symmetries of the system. To demonstrate the wide range of applications for the PGF method, we calculate the Coulomb coupling between two colloidal QDs [Fig. 1(i)] and identify terms describing the monopole-monopole interaction as well as the dipole-dipole coupling between the two QDs, a very common approach [5,59], but without using an explicit analytic form of the Green's function.

Carriers in semiconductor QDs are confined in all spatial dimensions and show discrete energy states [59,60]. The electronic properties as well as the optical spectra of Coulomb coupled QDs are influenced by the Coulomb interaction [17,30]. Even if the wave functions of the QDs do not overlap, the Coulomb coupling between the QDs may have a significant impact. The Coulomb interaction between two QDs with nonoverlapping wave functions contains direct electrostatic monopole coupling between the electrons and the holes of the two QDs [29], as well as dipole-dipole coupling like the nonradiative Förster energy transfer [22,61] [cf. Fig. 1(i)], which induces exciton energy shifts [23,62] and excitation transfer between the QDs [63,64].

The Coulomb coupling of the QDs depends on the distance between the QDs and, in the case of Förster coupling, on the relative orientation of the interband transition dipole moments (cf. Fig. 3), which has a specific impact, e.g., on colloidal QDs in a solvent. The standard simplified form of the dipole-dipole coupling between two pointlike emitters in a homogenous medium reads [63,65]

$$V^{\mathrm{F}}_{\mathrm{s}} = \frac{1}{4\pi\varepsilon_0\varepsilon_r}\left(\frac{\boldsymbol{d}_1\cdot\boldsymbol{d}_2}{|\boldsymbol{R}|^3} - 3\frac{(\boldsymbol{d}_1\cdot\boldsymbol{R})(\boldsymbol{d}_2\cdot\boldsymbol{R})}{|\boldsymbol{R}|^5}\right), \tag{16}$$

with $\boldsymbol{R} = \boldsymbol{r}_1 - \boldsymbol{r}_2$ denoting the emitter's distance and $\boldsymbol{d}_i$ the dipole moment of the emitter i. Therefore, if different arrangements of the QDs are included, various coupling elements need to be calculated for all contributing configurations. However, since the distance between the QDs can be very small, we have to go beyond the point-dipole form of Eq. (16), as is done in Refs. [6,30,59].

If a spatially dependent dielectric function $\varepsilon(\boldsymbol{r})$ is included, e.g., for colloidal quantum dots in a solvent, a separation of the integrals in the Fourier domain cannot be applied straightforwardly. Therefore, the calculation of the two-particle Coulomb interaction, without assuming a specific symmetry, requires the evaluation of a six dimensional integral scaling as $\mathcal{O}(N^6)$. For reducing the numerical effort to $\mathcal{O}(N^3)$, the PGF method (Sec. III) can be used. While typically other approaches rely on specific properties of the system, such as a piecewise constant dielectric function [32], the PGF method can be used for an arbitrary Green's function.

To retrieve the monopole-monopole, monopole-dipole, and dipole-dipole contributions for couplings between separated nanostructures such as QDs, a Taylor series of the Coulomb interaction is carried out, with respect to the unit cells using the usual scale separation [63]. For our example, the electron wave functions are given in the envelope approximation as product of an envelope function $\xi(\boldsymbol{r})$ and a lattice periodic Bloch part $u(\boldsymbol{r})$ [6,13]: $\phi_i(\boldsymbol{r}) = \xi_i(\boldsymbol{r})u_i(\boldsymbol{r})$. After a scale separation of the spatial operators [6] into the position of the nth unit cell $\boldsymbol{R}_n$ and the variation inside the cell $\boldsymbol{s}_n$, the Green's function is expanded in both spatial arguments in a Taylor series:

$$G(\boldsymbol{R}_n + \boldsymbol{s}_n, \boldsymbol{R}_{n'} + \boldsymbol{s}_{n'})\Big|_{\substack{\tilde{\boldsymbol{s}}_n = 0\\ \tilde{\boldsymbol{s}}_{n'} = 0}} = G(\boldsymbol{R}_n, \boldsymbol{R}_{n'}) + \cdots$$

$$+ [\boldsymbol{s}_n \cdot \nabla_{\tilde{\boldsymbol{s}}_n} G(\boldsymbol{R}_n + \tilde{\boldsymbol{s}}_n, \boldsymbol{R}_{n'} + \tilde{\boldsymbol{s}}_{n'}\overset{\curvearrowleft}{)}\ \nabla_{\tilde{\boldsymbol{s}}_{n'}} \cdot \boldsymbol{s}_{n'}]_{\substack{\tilde{\boldsymbol{s}}_n = 0\\ \tilde{\boldsymbol{s}}_{n'} = 0}} + \cdots . \tag{17}$$

While the zeroth order of the Taylor expanded Green's function [first term in Eq. (17)] represents the monopole-monopole interaction, the term of first order in both arguments, $\boldsymbol{s}_n$ and $\boldsymbol{s}_{n'}$, constitutes the dipole-dipole coupling [second term in Eq. (17)] such as the dipole induced Förster coupling transfer. For the example, mixed terms of the monopole-dipole interaction are not included in Eq. (17), since for quantum dynamical calculations the terms will often be neglected in a rotating wave approximation [30], but can be included if necessary (e.g., for carrier multiplication). Terms of higher order in the Taylor expansion [63] are discarded here, but they can be included in principle in a similar way. We see, using the Green's function formalism, the monopole-monopole as well as the dipole-dipole contributions can be identified without specifying a closed analytic expression for the Green's function [cf. Fig. 2(b)].

We start our analysis with the monopole-monopole Coulomb interaction between the two QDs, represented by the first term of Eq. (17). We assume, that the Green's function $G(\boldsymbol{r},\boldsymbol{r}')$ does not change significantly on the scale of the unit cell. Therefore, by using the normalization condition of the Bloch wave functions over a unit cell volume [30], $\frac{1}{V_{\mathrm{UC}}}\int_{\mathrm{UC}} d^3 s_n u_i^*(\boldsymbol{s}_n) u_j(\boldsymbol{s}_n) = \delta^{\lambda}_{ij}\delta^{\sigma}_{ij}$, the Coulomb elements of the monopole-monopole interaction V^{m}_{1234} read

$$V^{\mathrm{m}}_{1234} = e^2 \int d^3 r \int d^3 r' \xi_1^*(\boldsymbol{r})\xi_2^*(\boldsymbol{r}')G(\boldsymbol{r},\boldsymbol{r}') \times \xi_3(\boldsymbol{r}')\xi_4(\boldsymbol{r})\delta^{\lambda}_{14}\delta^{\sigma}_{14}\delta^{\lambda}_{23}\delta^{\sigma}_{23}. \tag{18}$$

The Kronecker δ's ensure the selection rules of band index λ and spin σ with respect to the QD indices.

For applications of the PGF method presented in Sec. III, Poisson equations for the different orders in the Taylor expansion Eq. (17) need to be formulated; cf. Fig. 2(c)(i). The Poisson equation for the scalar potential of the monopole-monopole coupling $\Phi^{\mathrm{m}}_{23}(\boldsymbol{r})$ is

$$\nabla_{\boldsymbol{r}} \cdot \big(\varepsilon(\boldsymbol{r})\nabla_{\boldsymbol{r}}\Phi^{\mathrm{m}}_{23}(\boldsymbol{r})\big) = -e\frac{\xi_2^*(\boldsymbol{r})\xi_3(\boldsymbol{r})}{\varepsilon_0}. \tag{19}$$

Note that $\Phi^{\mathrm{m}}_{23}(\boldsymbol{r})$ depends on the multi-indices 2 and 3 of the QD states and Eq. (19) is solved by the same Green's function $G(\boldsymbol{r},\boldsymbol{r}')$ as Eq. (13). In the case of monopole-monopole Coulomb coupling, the scalar potential Φ^{m}_{23} is determined by a product of the QD's envelope functions ξ_2 and ξ_3. Following the approach of the PGF method (Sec. III), the numerical solution of the Poisson Eq. (19) [cf. Fig. 2(d)(i)] is used to calculate the monopole-monopole Coulomb coupling elements:

$$V^{\mathrm{m}}_{1234} = e\int d^3 r\, \xi_1^*(\boldsymbol{r})\Phi^{\mathrm{m}}_{23}(\boldsymbol{r})\xi_4(\boldsymbol{r})\delta^{\lambda}_{14}\delta^{\sigma}_{14}\delta^{\lambda}_{23}\delta^{\sigma}_{23}. \tag{20}$$

Note that singularities of the Green's function are avoided, which are often difficult to treat numerically.

The dipole-dipole Coulomb coupling between two QDs (in principle the Förster induced excitation energy transfer) is described by the second term of the Taylor expanded Green's function in Eq. (17). To follow the PGF method, depicted in Fig. 2(i), a Poisson equation for the scalar potential of the dipole interaction Φ^{d}_{23} has to be identified, which is not as simple as in the monopole-monopole case. Therefore, an integration by parts is used, under the assumption of a vanishing boundary integral. The resulting Coulomb elements of the dipole-dipole interaction are

$$V^{\mathrm{d}}_{1234} = \int d^3 r \int d^3 r' \nabla_{\boldsymbol{r}} \cdot \big(\xi_1^*(\boldsymbol{r})\boldsymbol{d}_{14}\xi_4(\boldsymbol{r})\big) \times G(\boldsymbol{r},\boldsymbol{r}')\nabla_{\boldsymbol{r}'} \cdot \big(\xi_2^*(\boldsymbol{r}')\boldsymbol{d}_{23}\xi_3(\boldsymbol{r}')\big)\delta^{\sigma}_{14}\delta^{\sigma}_{23}, \tag{21}$$

including the microscopic interband transition dipole moments $\boldsymbol{d}_{ij}$ given by the Bloch functions of the unit cells as [56,63]

$$\boldsymbol{d}_{ij} = \frac{1}{V_{\mathrm{UC}}}\int_{\mathrm{UC}} d^3 s_n u_i^*(\boldsymbol{s}_n)\boldsymbol{s}_n u_j(\boldsymbol{s}_n). \tag{22}$$

Note that the interband transition elements $\boldsymbol{d}_{ij}$, which appear during the usual scale separation, depend on the spin configurations [66] of the QD states i and j. The generalized scalar potential $\Phi^{\mathrm{d}}_{23}(\boldsymbol{r})$ of the Coulomb dipole interaction of a QD is determined by the generalized Poisson equation [cf. Fig. 2(c)(i)]:

$$\nabla_{\boldsymbol{r}} \cdot \big(\varepsilon(\boldsymbol{r})\nabla_{\boldsymbol{r}}\Phi^{\mathrm{d}}_{23}(\boldsymbol{r})\big) = \frac{\nabla_{\boldsymbol{r}} \cdot (\xi_2^*(\boldsymbol{r})\boldsymbol{d}_{23}\xi_3(\boldsymbol{r}))}{\varepsilon_0}, \tag{23}$$

induced by the dipole distribution, which includes the QD's envelope functions ξ_2 and ξ_3 and the microscopic interband transition dipole moment $\boldsymbol{d}_{23}$. Therefore, the scalar potential $\Phi^{\mathrm{d}}_{23}(\boldsymbol{r})$ has a different unit than the scalar potential of the monopole-monopole coupling $\Phi^{\mathrm{m}}_{23}(\boldsymbol{r})$ in Eq. (19). Using the PGF method, the generalized scalar potential Φ^{d}_{23} is obtained numerically from the Poisson Eq. (23) [cf. Fig. 2(d)(i)] and, therefore, the Coulomb coupling elements of the dipole-dipole interaction V^{d}_{1234} can be written as

$$V^{\mathrm{d}}_{1234} = \int d^3 r \big(\nabla_{\boldsymbol{r}} \cdot (\xi_1^*(\boldsymbol{r})\boldsymbol{d}_{14}\xi_4(\boldsymbol{r}))\Phi^{\mathrm{d}}_{23}(\boldsymbol{r})\delta^{\sigma}_{14}\delta^{\sigma}_{23}\big). \tag{24}$$

Equation (23) and Eq. (24) together describe the influence of the dipole distribution on Coulomb coupled QDs in a specific spatial arrangement. Hence, as Fig. 3 illustrates, the Coulomb coupling elements of the dipole-dipole interaction are not only a function of the distance between the QDs [63] but also on their spatial dipole orientation [30].

The PGF method allowed us to calculate the monopole-monopole and dipole-dipole parts separately. For both contributions, the generalized scalar potential is calculated for a specific generalized Poisson equation. We showed that, based on the Taylor expansion of the Green's function, the Coulomb coupling elements of the monopole-monopole as well as the dipole-dipole contribution of the Coulomb interaction can be calculated numerically efficiently without being restricted to specific symmetries or permittivities by using an adapted Poisson equation.

V. COUPLING TO CONTINUUM STATES

We demonstrate, that the PGF method can also be applied with great benefit, if specific symmetries are considered, which simplify the Coulomb coupling elements calculation [depicted in Fig. 2(ii)]. Therefore, we will present the rotationally symmetric Coulomb coupling between bound quantum dot states and many continuum states in a spatially homogenous medium with a constant dielectric function ε_r.

In a variety of many-body systems, a finite number of localized discrete energy states is coupled via Coulomb interaction to a continuum of states from an embedding system. As an important example we investigate the Coulomb coupling $V^{cvvc}_{kjjk'}$ between a hole in a bound QD valence band of state v,j, which is localized inside the QD, and an electron in a free continuum state $\boldsymbol{k}$ of the conduction band c (e.g., of an embedding carrier reservoir) [67]; cf. Fig. 1(ii). Other examples, which can be calculated in a similar way, are impurities in a bulk medium or other nanostructures such as quantum wells [68] and wires [69], as well as molecular systems [24,70].

The unbound continuum states in a bulk semiconductor are characterized by a three dimensional wave vector $\boldsymbol{k}$ and a band index λ. The calculation of the Coulomb interaction between a bound state in a QD and many continuum states in the embedding material [29] requires the calculation of a large number of coupling elements. Typically, in pure bulk materials, electron wave functions are expanded in plane waves. Since the presence of the QD confinement potential modifies the continuum wave functions, a description beyond the plane wave approximation may be necessary [27,31]. Therefore, the PGF method, presented in Sec. III, can be used to efficiently calculate Coulomb coupling elements for modified continuum wave functions. To get a consistent set of wave functions (bound QD wave functions as well as unbound continuum wave functions), the radial Schrödinger differential equation is solved using a finite element method (FEM) solver [67]. The radially symmetric QD confinement potential is assumed to be of the form $V(r) = V_0/(\cosh^2(\frac{r}{a}))$, with height V_0 and extension a. Due to the radial symmetry, the unbound continuum states can be described by a one dimensional wave vector k.

If the confinement potential is rotationally symmetric, spherical coordinates can be used to simplify the calculation of the Coulomb coupling. Therefore, the envelopes of the electron wave functions are decomposed into a product of radial parts $R^l(r)$ and a spherical harmonic $Y^l_m(\vartheta,\varphi)$, with l denoting the angular momentum number and m the magnetic quantum number: $\xi(\boldsymbol{r}) = R^l(r)Y^l_m(\vartheta,\varphi)$.

For a formulation of the PGF method in spherical coordinates, the Green's function is separated into a radial part $g^l(r,r')$ [71] and spherical harmonics [13,22]:

$$G(\boldsymbol{r},\boldsymbol{r}') = \sum_{lm} \frac{1}{\varepsilon_0\varepsilon_r} Y^{l*}_m(\vartheta,\varphi)Y^l_m(\vartheta',\varphi')g^l(r,r'). \tag{25}$$

To specify the calculation to the Coulomb coupling between the QD ground state and unbound states of the continuum, the charge density is determined by the QD ground state wave function. Since the angular momentum of the bound ground state in the QD is $l = 0$, the charge density reads $\varrho^0_{23}(\boldsymbol{r}) = \frac{e}{4\pi} R^{0*}_2(r)R^0_3(r)$. To follow the approach of the PGF method, in case of a radially symmetric confinement potential, the Green's function, given by Eq. (25), and the charge density are used to express the scalar potential $\Phi_{23}(\boldsymbol{r})$ in spherical coordinates [cf. Eq. (12), Fig. 2(ii)]. Evaluating the spherical contributions of Eq. (25), the radial scalar potential is formally given by

$$\Phi^0_{23}(r) = \frac{e}{4\pi\varepsilon_0\varepsilon_r} \int dr' r'^2 R^{0*}_2(r')g^0(r,r')R^0_3(r'). \tag{26}$$

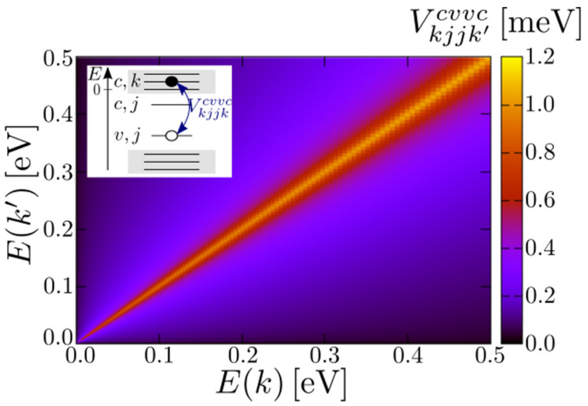

FIG. 4. Bound-to-continuum Coulomb coupling $V^{cvvc}_{kjjk'}$ of a hole in the QD valence band state j and an electron in the continuum conduction band states k. The Coulomb coupling starts at the energy of the energetic lowest continuum state. To reach numerical convergence, a high number of Coulomb coupling elements need to be calculated, since they couple to many continuum states of the embedding carrier reservoir.

Note that Eq. (26) represents the equivalent to Eq. (12) for the radially symmetric case. Thus, analogous to the Poisson Eq. (13) [cf. Fig. 2(c)] for a spatially homogenous medium ε_r, the Laplace operator $\Delta_{\boldsymbol{r}}$ in spherical coordinates with momentum $l = 0$ appears and the Poisson equation for the radially symmetric problem reads

$$\left(\frac{\partial^2}{\partial r^2} + \frac{2}{r}\frac{\partial}{\partial r}\right)\Phi^0_{23}(r) = -e\frac{R^{0*}_2(r)R^0_3(r)}{4\pi\varepsilon_0\varepsilon_r}. \tag{27}$$

In the approach of the PGF method, the radial part of the scalar potential $\Phi^0_{23}(r)$, which is obtained by a numerical solution of Eq. (27) [cf. Fig. 2(d)(ii)], is used to calculate the Coulomb coupling elements for a radially symmetric problem, analogous to Eq. (20):

$$V_{1234} = e\int dr\, r^2 R^{l*}_1(r)\Phi^0_{23}(r)R^l_4(r)\delta^\lambda_{14}\delta^\sigma_{14}\delta^\lambda_{23}\delta^\sigma_{23}\delta^l_{14}\delta^m_{14}. \tag{28}$$

Note that the angular part of the electron wave functions for the Coulomb coupling elements in Eq. (28) is determined by spherical harmonics [cf. Eq. (25)] and, therefore, it is calculated analytically.

In the case of a radially symmetric confinement potential, the computational requirements for calculating Coulomb coupling elements are significantly reduced, since Eq. (28) only requires the evaluation of a one dimensional spatial integral [cf. Fig. 2(e)(ii)]. The resulting Coulomb coupling elements $V^{cvvc}_{kjjk'}$, depicted in Fig. 4, are relevant for the formation of bound-to-continuum excitons [29].

We show in Fig. 1(ii) the Coulomb coupling between the QD ground state and the continuum states starting at the energy of the lowest continuum state. The most relevant contribution is on the diagonal $k = k'$; cf. Fig. 4. Since the continuum states are only occupied near the energy minimum of continuum levels and the coupling to the QD's resonances decreases, the number of continuum states in numerical calculations is finite [27]. However, to reach numerical convergence, a high number of coupling elements needs to be calculated [29].

We used the PGF method for an efficient numerical calculation of bound-to-continuum Coulomb coupling elements. Moreover, we have shown that the PGF method can also exploit symmetries to further reduce the computational cost for calculating Coulomb coupling elements.

VI. CONCLUSION

We presented a numerical method, based on a Green's function representation of the solution of a generalized Poisson equation, to calculate Coulomb coupling elements efficiently by decreasing the number of integrals in the two-particle Coulomb interaction. The Poisson Green's function method can be applied to a broad range of applications, since the method is not restricted to specific symmetries of the potential or the wave functions. Furthermore, a spatially inhomogeneous dielectric function can be included by using the solution of a generalized Poisson equation. Thus the influence of a medium and, e.g., surface charge effects can be included.

We demonstrate the strength of the formalism, particularly with regard to the calculation of a high number of Coulomb coupling elements, by presenting two applications of the method in real space: the spatially dependent interdot coupling between two QDs and the coupling of a QD to many continuum states. By expanding the Green's function of two Coulomb coupled QDs in a Taylor series, an identification of terms connected to the monopole-monopole and the dipole-dipole interaction is possible without using an explicit analytic form of the Green's function. Though the presented method does not prevent the application of commonly used simplifications. In the case of radial symmetry, the reduction of the computational time can be huge, since only a one dimensional differential equation needs to be solved and one spatial integral needs to be evaluated. Accordingly, the Poisson Green's function method presents a general approach to increase the computational efficiency in numerical calculations of Coulomb coupling elements.

ACKNOWLEDGMENTS

We thank Andreas Knorr and T. Sverre Theuerholz for insightful discussions. Financial support by Deutsche Forschungsgemeinschaft (DFG) through the Research Training Group GRK 1558 (A.Z.) and through the SFB 787 (S.K.) is gratefully acknowledged. M.R. also acknowledges support through the SFB 951.

[1] D. Nikonov, A. Imamoğlu, L. Butov, and H. Schmidt, Phys. Rev. Lett. **79**, 4633 (1997).

[2] T. R. Nielsen, P. Gartner, M. Lorke, J. Seebeck, and F. Jahnke, Phys. Rev. B **72**, 235311 (2005).

[3] D. Reuter, P. Kailuweit, A. D. Wieck, U. Zeitler, O. Wibbelhoff, C. Meier, A. Lorke, and J. C. Maan, Phys. Rev. Lett. **94**, 026808 (2005).

[4] V. A. Fonoberov, E. P. Pokatilov, and A. A. Balandin, Phys. Rev. B **66**, 085310 (2002).

[5] K. Gawarecki, M. Pochwała, A. Grodecka-Grad, and P. Machnikowski, Phys. Rev. B **81**, 245312 (2010).

[6] P. Machnikowski and E. Rozbicki, Phys. Status Solidi B **246**, 320 (2009).

[7] W. W. Chow, H. C. Schneider, and M. C. Phillips, Phys. Rev. A **68**, 053802 (2003).

[8] I. F. Herbut, V. Juričić, and O. Vafek, Phys. Rev. Lett. **100**, 046403 (2008).

[9] E. Malic, T. Winzer, E. Bobkin, and A. Knorr, Phys. Rev. B **84**, 205406 (2011).

[10] T. Kitae, T. Nakayama, and K. Kano, J. Chem. Soc., Perkin Trans. 2, 207 (1998).

[11] M. C. Strain, G. E. Scuseria, and M. J. Frisch, Science **271**, 51 (1996).

[12] A. Franceschetti and A. Zunger, Phys. Rev. Lett. **78**, 915 (1997).

[13] P. Kowalski, L. Marcinowski, and P. Machnikowski, Phys. Rev. B **87**, 075309 (2013).

[14] H. C. Schneider, W. W. Chow, and S. W. Koch, Phys. Rev. B **64**, 115315 (2001).

[15] A. Franceschetti and A. Zunger, Phys. Rev. B **62**, 2614 (2000).

[16] T. Miyake and F. Aryasetiawan, Phys. Rev. B **77**, 085122 (2008).

[17] W. Hoyer, M. Kira, and S. W. Koch, Phys. Rev. B **67**, 155113 (2003).

[18] N. Baer, S. Schulz, P. Gartner, S. Schumacher, G. Czycholl, and F. Jahnke, Phys. Rev. B **76**, 075310 (2007).

[19] C. Sieh, T. Meier, F. Jahnke, A. Knorr, S. W. Koch, P. Brick, M. Hübner, C. Ell, J. Prineas, G. Khitrova, and H. M. Gibbs, Phys. Rev. Lett. **82**, 3112 (1999).

[20] J. Wühr, V. M. Axt, and T. Kuhn, Phys. Rev. B **70**, 155203 (2004).

[21] G. Cantele, D. Ninno, and G. Iadonisi, Phys. Rev. B **64**, 125325 (2001).

[22] A. Nazir, B. W. Lovett, S. D. Barrett, J. H. Reina, and G. A. Briggs, Phys. Rev. B **71**, 045334 (2005).

[23] Y. Zelinskyy, Y. Zhang, and V. May, J. Phys. Chem. A **116**, 11330 (2012).

[24] J. M. Daniels, P. Machnikowski, and T. Kuhn, Phys. Rev. B **88**, 205307 (2013).

[25] L. F. Greengard and J. Huang, J. Comput. Phys. **180**, 642 (2002).

[26] R. Ferreira and G. Bastard, Nanoscale Res. Lett. **1**, 120 (2006).

[27] S. C. Kuhn and M. Richter, Phys. Rev. B **91**, 155309 (2015).

[28] A. Steinhoff, P. Gartner, M. Florian, and F. Jahnke, Phys. Rev. B **85**, 205144 (2012).

[29] S. C. Kuhn and M. Richter, Phys. Rev. B **90**, 125308 (2014).

[30] J. F. Specht, A. Knorr, and M. Richter, Phys. Rev. B **91**, 155313 (2015).

[31] T. R. Nielsen, P. Gartner, and F. Jahnke, Phys. Rev. B **69**, 235314 (2004).

[32] B. Pasenow, M. Reichelt, T. Stroucken, T. Meier, and S. W. Koch, Phys. Rev. B **71**, 195321 (2005).

[33] L. D. Hallam, J. Weis, and P. A. Maksym, Phys. Rev. B **53**, 1452 (1996).

[34] S. Balay, S. Abhyankar, M. F. Adams, J. Brown, P. Brune, K. Buschelman, L. Dalcin, V. Eijkhout, W. D. Gropp, D. Kaushik, M. G. Knepley, L. C. McInnes, K. Rupp, B. F. Smith, S. Zampini,

and H. Zhang, PETSc Users Manual, Tech. Rep. ANL-95/11 - Revision 3.6, Argonne National Laboratory (2015).
[35] Y. Notay and A. Napov, J. Comput. Phys. **281**, 237 (2015).
[36] T. Guillet and R. Teyssier, J. Comput. Phys. **230**, 4756 (2011).
[37] M. Stopa, Physica B **249-251**, 228 (1998).
[38] J. Sée, P. Dollfus, and S. Galdin, J. Appl. Phys. **92**, 3141 (2002).
[39] A. Franceschetti, A. Williamson, and A. Zunger, J. Phys. Chem. B **104**, 3398 (2000).
[40] M. A. Watson, Y. Kurashige, T. Nakajima, and K. Hirao, J. Chem. Phys. **128**, 054105 (2008).
[41] F. R. Manby and P. J. Knowles, Phys. Rev. Lett. **87**, 163001 (2001).
[42] L. Robledo, J. Elzerman, G. Jundt, M. Atatüre, A. Högele, S. Fält, and A. Imamoglu, Science **320**, 772 (2008).
[43] V. I. Klimov, S. A. Ivanov, J. Nanda, M. Achermann, I. Bezel, J. A. McGuire, and A. Piryatinski, Nature (London) **447**, 441 (2007).
[44] M. Reichelt, B. Pasenow, T. Meier, T. Stroucken, and S. W. Koch, Phys. Rev. B **71**, 035346 (2005).
[45] W. Vogel, D.-G. Welsch, and S. Wallentowitz, *Quantum Optics An Introduction* (WILEY-VCH, New York, 2001).
[46] M. Wubs, L. G. Suttorp, and A. Lagendijk, Phys. Rev. A **68**, 013822 (2003).
[47] A. Tip, Phys. Rev. A **56**, 5022 (1997).
[48] A. J. Williamson, L. W. Wang, and A. Zunger, Phys. Rev. B **62**, 12963 (2000).
[49] M. I. Stockman, D. J. Bergman, and T. Kobayashi, Phys. Rev. B **69**, 054202 (2004).
[50] S. R. White, J. W. Wilkins, and M. P. Teter, Phys. Rev. B **39**, 5819 (1989).
[51] E. Antillon, B. Wehefritz-Kaufmann, and S. Kais, Phys. Rev. E **85**, 036706 (2012).
[52] Y. Nishimura, Z. Lin, J. Lewandowski, and S. Ethier, J. Comput. Phys. **214**, 657 (2006).
[53] E. L. Briggs, D. J. Sullivan, and J. Bernholc, Phys. Rev. B **54**, 14362 (1996).
[54] O. Ayala and L.-P. Wang, Parallel Comput. **39**, 58 (2012).
[55] L. Füsti-Molnár, J. Chem. Phys. **119**, 11080 (2003).
[56] I. V. Solovyev and M. Imada, Phys. Rev. B **71**, 045103 (2005).
[57] J. Heyd, G. E. Scuseria, and M. Ernzerhof, J. Chem. Phys **118**, 8207 (2003).
[58] S. A. Khrapak, A. V. Ivlev, G. E. Morfill, and S. K. Zhdanov, Phys. Rev. Lett. **90**, 225002 (2003).
[59] J. Danckwerts, K. J. Ahn, J. Förstner, and A. Knorr, Phys. Rev. B **73**, 165318 (2006).
[60] V. I. Klimov, A. A. Mikhailovsky, D. W. McBranch, C. A. Leatherdale, and M. G. Bawendi, Science **287**, 1011 (2000).
[61] T. S. Theuerholz, A. Carmele, M. Richter, and A. Knorr, Phys. Rev. B **87**, 245313 (2013).
[62] D. Ziemann and V. May, J. Phys. Chem. Lett. **5**, 1203 (2014).
[63] R. Baer and E. Rabani, J. Chem. Phys. **128**, 184710 (2008).
[64] B. W. Lovett, J. H. Reina, A. Nazir, and G. A. D. Briggs, Phys. Rev. B **68**, 205319 (2003).
[65] G. Kyas and V. May, J. Chem. Phys **134**, 034701 (2011).
[66] G. D. Scholes and D. L. Andrews, Phys. Rev. B **72**, 125331 (2005).
[67] S. C. Kuhn, A. Knorr, M. Richter, N. Owschimikow, M. Kolarczik, Y. I. Kaptan, and U. Woggon, Phys. Rev. B **89**, 201414 (2014).
[68] H. T. Duc, J. Förstner, and T. Meier, Phys. Rev. B **82**, 115316 (2010).
[69] I. Affleck and P. Simon, Phys. Rev. Lett. **86**, 2854 (2001).
[70] H. J. Krenner, M. Sabathil, E. C. Clark, A. Kress, D. Schuh, M. Bichler, G. Abstreiter, and J. J. Finley, Phys. Rev. Lett. **94**, 057402 (2005).

[71] Often, the Coulomb interaction is represented by the Green's function generated in a spatially homogenous medium [12,22]:

$$G(\boldsymbol{r},\boldsymbol{r}') = \frac{1}{4\pi\varepsilon_0\varepsilon_r}\frac{1}{|\boldsymbol{r}-\boldsymbol{r}'|}. \qquad (29)$$

Expanding the Green's function in terms of Legendre polynomials, the radial part with angular momentum l reads

$$g^l(r,r') = \frac{1}{2l+1}\left(\frac{r'^l}{r^{l+1}}\Theta(r'-r) + \frac{r^l}{r'^{l+1}}\Theta(r-r')\right), \qquad (30)$$

which includes the Heaviside step function $\Theta(r-r')$.